

This article appeared in a journal published by Elsevier. The attached copy is furnished to the author for internal non-commercial research and education use, including for instruction at the authors institution and sharing with colleagues.

Other uses, including reproduction and distribution, or selling or licensing copies, or posting to personal, institutional or third party websites are prohibited.

In most cases authors are permitted to post their version of the article (e.g. in Word or Tex form) to their personal website or institutional repository. Authors requiring further information regarding Elsevier's archiving and manuscript policies are encouraged to visit:

<http://www.elsevier.com/copyright>



An efficient numerical method of Landau–Brazovskii model

Pingwen Zhang^{*}, Xinwei Zhang

LMAM and School of Mathematical Sciences, Peking University, Beijing 100871, People's Republic of China

Received 30 September 2007; received in revised form 10 January 2008; accepted 14 February 2008

Available online 29 February 2008

Abstract

Using the Landau–Brazovskii model, a new numerical implementation is developed to investigate the phase behavior of the diblock copolymer system. Though the method is based on the Fourier expansion of order parameter, a priori symmetric information is not required, and more significantly, the period structure can be adjusted automatically during the iteration as well. The method enables us to calculate the phase diagram, discover new meta-stable phases, validate the epitaxial relation in the phase transition process, and find the inefficiency of the Landau–Brazovskii model for some situations.

© 2008 Elsevier Inc. All rights reserved.

Keywords: Landau–Brazovskii model; Fourier space method; Phase diagram; Meta-stable phase; Epitaxial relation

1. Introduction

During the last decades, diblock copolymers have attracted a lot of attention of many polymer specialists because of their various and abundant microstructures. A typical molecule of a diblock copolymer consists of two incompatible blocks, and each block is a long chain composed of a lot of the same monomers. As the result of the incompatibility between the two blocks, the blocks tend to separate when the temperature is low, but they cannot be separated at a macroscopic scale because they remain connected at one point. This kind of separation can not be observed in the macroscale, but can form microstructures at the molecular level. At different temperatures, different microstructures form because of the competition between the system's internal energy and the entropy. Lamellar, cylinder, sphere and gyroid phases are usually observed, and perforated-lamellar, double-diamond phases are occasionally observed in the experiments since they are meta-stable.

Theoretically, the phase behavior of a diblock copolymer system is studied through mean-field theory. A good review on this is given by Matsen [1]. Mean-field theory has been a powerful tool for studying phase behavior since van der Waals developed the revised equation of state though he did not realize it is a kind

^{*} Corresponding author. Tel.: +86 10 6275 9851; fax: +86 10 6276 7146.

E-mail addresses: pzhang@pku.edu.cn (P. Zhang), xinwei@zhang.net (X. Zhang).

URL: <http://www.math.pku.edu.cn/pzhang> (P. Zhang).

of mean-field approximation. A well-known example is the Ising model, which explains the ferromagnetic phase transition very well. Using the Gaussian molecular model invented by Doi and Edwards [2], Helfand developed self-consistent mean-field theory (SCFT) for diblock copolymer systems [4,5]. Taking a different approach, Leibler [6] expanded the free energy near the disordered phase, and found a Landau expansion in weakly-segregated melts, and predicted the lamellar, hexagonal and body-centered cubic phases. By approximating the second and higher order vertex functions of Leibler's model, Landau–Brazovskii model [7] could be derived. This model provides a framework for systems that are undergoing a phase transition driven by a short-wave length instability between the disordered phases and the ordered phases. Besides the major contribution on the fluctuation effects in the theory of microphase separation in block copolymers, Fredrickson and Helfand [8] also found the relationship between Leibler weak-segregation theory and the Landau–Brazovskii model by mapping the former onto the latter.

Numerically, the mean-field methods can be classified into two categories. The first is calculated in Fourier space by expanding the order parameter in a finite set of basis functions under an assumption of symmetry. The symmetry itself determines the morphology of the solutions. Using such a method, Matsen and Schick [9] first calculated a predicted phase diagram for diblock copolymer systems under SCFT, and their results are consistent with the work of Leibler [6]. The second type is calculated in real space. A typical implementation was developed by Drolet and Fredrickson [10] and was later improved by Tzeremes et al. [11]. The advantage of real space methods is that they do not require a priori assumption of symmetry, but this lack of the symmetry information significantly increases the computational complexity.

Research on the phase diagram of the equilibrium states and the stability of the possible microstructures are both important. Shi et al. [12] developed a general theoretical framework for the study of anisotropic composition fluctuations about an ordered block copolymer phase by expanding the free energy around the ordered phase and investigating the band structure of the system. An application on the lamellar phase was proved to be successful. Under the same framework, Shi [13] investigated the spinodal phenomenon from the hexagonal phase to lamellar phase and the hexagonal phase to sphere phase using the Landau–Brazovskii model.

Though the numerical methods in both Fourier space and real space have been successfully applied to calculate the structure of the phases, both have disadvantages. Since the Fourier space methods assume both information about the period structure and the symmetry, the structure of the solution must be known initially. As a result, these methods can be used to generate phase diagrams, but cannot be used to discover new stable or meta-stable phases. For the real space methods, the calculation area must be set initially. While the calculation area is normally set as a cube in 3-D problems and a square in 2-D problems, the period of one ordered phase is not likely to be a cube or a square. To dilute the influence of this mismatch, the calculation area has to be set as large as possible. This, however, dramatically increases the computational complexity. By applying the Landau–Brazovskii model, this research tries to plant the advantages of the real space methods into the Fourier space ones to create a method that does not need a priori information about symmetry. Another important contribution of the method is that the period vectors are treated as variables just like the order parameter, so they will be automatically adjusted during iterations.

Before we can go further, a short introduction of the Landau–Brazovskii model is necessary. In general, a system undergoing the phase transition can be described by a free energy functional $f(\{\phi\})$ which depends on a set of order parameters $\{\phi\}$. In the Landau–Brazovskii model, the free energy density functional is given by

$$f(\phi(\mathbf{r})) = \frac{1}{V} \int d\mathbf{r} \left\{ \frac{\xi_0^2}{8q_0^2} [(\nabla^2 + q_0^2)\phi(\mathbf{r})]^2 + \frac{\tau}{2} [\phi(\mathbf{r})]^2 - \frac{\gamma}{3!} [\phi(\mathbf{r})]^3 + \frac{\lambda}{4!} [\phi(\mathbf{r})]^4 \right\}. \quad (1.1)$$

In Eq. (1.1), $\phi(\mathbf{r})$ is the order parameter, which is the density deviation of a kind of monomer from the disordered phase; V is the system volume; ξ_0 is the bare correlation length; q_0 is the critical wave length; τ is the reduced temperature; and γ and $\lambda > 0$ are phenomenological constants. For simplification, we rescale the length and the energy unit to $1/q_0$ and λ , respectively, and define the rescaled quantities as

$$\tilde{f} = \frac{f}{\lambda}, \quad \tilde{\xi} = \frac{q_0 \xi_0^2}{4\lambda}, \quad \tilde{\tau} = \frac{\tau}{\lambda}, \quad \tilde{\gamma} = \frac{\gamma}{\lambda}, \quad \tilde{\phi}(\tilde{\mathbf{r}}) = \phi(q_0 \mathbf{r}), \quad \tilde{V} = q_0^3 V.$$

The free energy density function then becomes

$$f(\tilde{\phi}(\tilde{\mathbf{r}})) = \frac{1}{V} \int d\mathbf{r} \left\{ \frac{\xi^2}{2} [(\nabla^2 + 1)\tilde{\phi}(\tilde{\mathbf{r}})]^2 + \frac{\tilde{\tau}}{2} [\tilde{\phi}(\tilde{\mathbf{r}})]^2 - \frac{\tilde{\gamma}}{3!} [\tilde{\phi}(\tilde{\mathbf{r}})]^3 + \frac{1}{4!} [\tilde{\phi}(\tilde{\mathbf{r}})]^4 \right\}. \quad (1.2)$$

Because all the discussion what follows focuses on the rescaled quantities, we will neglect the tilde. For ordered phases, the order parameters $\phi^{(0)}$ are periodic functions which minimize the free energy density functional, which means

$$\left. \frac{\delta f}{\delta \phi(\mathbf{r})} \right|_{\phi^{(0)}} = 0. \quad (1.3)$$

Our goal is to identify as many periodic functions $\phi(\mathbf{r})$ that satisfy Eq. (1.3) as possible, thereby revealing the phase behavior of this polymer system.

2. Numerical method description

As mentioned above, the period vectors are also treated as variables in the method, we need to add them to the free energy density function. Before we do this, a brief introduction to the Bravais lattice and reciprocal lattice is necessary. For any d -dimensional period structure $F(\mathbf{r})$, $\mathbf{r} \in \mathcal{R}^d$, the repeated structural unit is called a unit cell. A primitive unit cell, described by d vectors $\mathbf{a}_1, \mathbf{a}_2, \dots, \mathbf{a}_d$, has the smallest possible volume. The Bravais lattice is then defined by

$$\mathbf{R}_l = l_1 \mathbf{a}_1 + l_2 \mathbf{a}_2 + \dots + l_d \mathbf{a}_d,$$

where $\mathbf{l} = (l_1, \dots, l_d)$ is a d -dimensional vector with components $l_i \in \mathcal{Z}$. For any \mathbf{R}_l in the Bravais lattice, the structure is invariant under a lattice translation, which means $F(\mathbf{r} + \mathbf{R}_l) = F(\mathbf{r})$.

Given the primitive vectors $(\mathbf{a}_1, \mathbf{a}_2, \dots, \mathbf{a}_d)$, the primitive reciprocal vectors $(\mathbf{b}_1, \mathbf{b}_2, \dots, \mathbf{b}_d)$ satisfy the equation $\mathbf{a}_i \cdot \mathbf{b}_j = 2\pi\delta_{ij}$. The reciprocal lattice is then specified by

$$\mathbf{G}_l = l_1 \mathbf{b}_1 + l_2 \mathbf{b}_2 + \dots + l_d \mathbf{b}_d,$$

where $\mathbf{l} = (l_1, \dots, l_d)$ is a d -dimensional vector with components $l_i \in \mathcal{Z}$. One of the most important applications of the reciprocal lattice is that plane waves $\{e^{i\mathbf{G} \cdot \mathbf{r}}\}$ are a set of basis functions for any function with period $\mathbf{a}_1, \mathbf{a}_2, \dots, \mathbf{a}_d$.

Without loss of generality, we will discuss the three-dimensional problem thereafter. The primitive vectors are denoted by $\mathbf{a}_1 = (a_{11}, a_{12}, a_{13})$, $\mathbf{a}_2 = (a_{21}, a_{22}, a_{23})$, $\mathbf{a}_3 = (a_{31}, a_{32}, a_{33})$, and the primitive reciprocal vectors are denoted by $\mathbf{b}_1 = (b_{11}, b_{12}, b_{13})$, $\mathbf{b}_2 = (b_{21}, b_{22}, b_{23})$, $\mathbf{b}_3 = (b_{31}, b_{32}, b_{33})$; and $\{\mathbf{G}\} = \{\mathbf{G}_{mnk} | \mathbf{G}_{mnk} = m\mathbf{b}_1 + n\mathbf{b}_2 + k\mathbf{b}_3\}$, where $m, n, k \in \mathcal{Z}$, are the reciprocal lattice. For convenience, element of $\{\mathbf{G}\}$ is sometimes written as \mathbf{G}_i , $i \in \mathcal{Z}$ instead of \mathbf{G}_{mnk} .

Because the equilibrium phases are periodic, the free energy density function depends not only on $\phi(\mathbf{r})$ but also on the primitive lattice. It can be calculated by dividing the free energy in a primitive unit cell Ω by its volume.

$$f(\phi(\mathbf{r}), \mathbf{a}_1, \mathbf{a}_2, \mathbf{a}_3) = \frac{1}{V} \int_{\Omega} d\mathbf{r} \left\{ \frac{\xi^2}{2} [(\nabla^2 + 1)\phi(\mathbf{r})]^2 + \frac{\tau}{2} [\phi(\mathbf{r})]^2 - \frac{\gamma}{3!} [\phi(\mathbf{r})]^3 + \frac{1}{4!} [\phi(\mathbf{r})]^4 \right\}, \quad (2.1)$$

where V is the volume of the primitive unit cell.

Because the order parameter $\phi(\mathbf{r})$ is periodic on the Bravais lattice, and the functions $\{e^{i\mathbf{G}_{mnk} \cdot \mathbf{r}}\}$, where $\mathbf{G}_{mnk} \in \{\mathbf{G}\}$, form a basis for the function space $\{h(\mathbf{r}) | h(\mathbf{r} + \mathbf{R}_l) = h(\mathbf{r})\}$, it can be specified as

$$\phi(\mathbf{r}) = \sum_{\{\mathbf{G}\}} \phi(\mathbf{G}) e^{i\mathbf{G} \cdot \mathbf{r}}. \quad (2.2)$$

The fact that $\phi(\mathbf{r})$ is a real function and that $\int d\mathbf{r} \phi(\mathbf{r}) = 0$ implies that the Fourier coefficients satisfy $\phi(-\mathbf{G}) = \phi^*(\mathbf{G})$ and $\phi(\mathbf{0}) = 0$.

Since for any $\mathbf{G}_1 + \mathbf{G}_2 + \dots + \mathbf{G}_m \neq \mathbf{0}$, $m \in \mathcal{N}$,

$$\int_{\Omega} e^{i(\mathbf{G}_1 + \mathbf{G}_2 + \dots + \mathbf{G}_m) \cdot \mathbf{r}} d\mathbf{r} = 0,$$

when substituting Eq. (2.2) into Eq. (2.1), the free energy density function becomes

$$\begin{aligned} f(\phi(\mathbf{r}), \mathbf{a}_1, \mathbf{a}_2, \mathbf{a}_3) &= f(\{\phi(\mathbf{G})\}, \mathbf{b}_1, \mathbf{b}_2, \mathbf{b}_3) \\ &= \sum_{\mathbf{G}} \frac{1}{2} [\xi^2 (1 - \mathbf{G}^2)^2 + \tau] \phi(\mathbf{G}) \phi(-\mathbf{G}) - \frac{\gamma}{3!} \sum_{\mathbf{G}_1 + \mathbf{G}_2 + \mathbf{G}_3 = \mathbf{0}} \phi(\mathbf{G}_1) \phi(\mathbf{G}_2) \phi(\mathbf{G}_3) + \frac{1}{4!} \\ &\quad \times \sum_{\mathbf{G}_1 + \mathbf{G}_2 + \mathbf{G}_3 + \mathbf{G}_4 = \mathbf{0}} \phi(\mathbf{G}_1) \phi(\mathbf{G}_2) \phi(\mathbf{G}_3) \phi(\mathbf{G}_4). \end{aligned} \quad (2.3)$$

In order to reach the equilibrium state, the problem requires a set of Fourier coefficients $\{\phi(\mathbf{G})\}$ and a primitive reciprocal vectors $\mathbf{b}_1, \mathbf{b}_2, \mathbf{b}_3$ that can minimize the free energy density. This can be separated into two problems.

1. Given $\mathbf{b}_1, \mathbf{b}_2, \mathbf{b}_3$, minimize the free energy density to generate $\{\phi(\mathbf{G})\}$.
2. Given a set of $\{\phi(\mathbf{G})\}$, find the vectors $\mathbf{b}_1, \mathbf{b}_2, \mathbf{b}_3$ to minimize the free energy density.

Both of the problems have to be satisfied simultaneously if $\{\phi(\mathbf{G})\}$ and $\mathbf{b}_1, \mathbf{b}_2, \mathbf{b}_3$ are solutions. Sections 2.1 and 2.2 will discuss the method to solve the above two problems, respectively.

In theory, the set of basis functions is infinite. In practice, however, the number of basis functions has to be finite, and we expand the order parameter $\phi(\mathbf{r})$ into N modes, which means

$$\phi(\mathbf{r}) \approx \phi^{(N)}(\mathbf{r}) = \sum_{m,n,k} \phi(\mathbf{G}_{mnk}) e^{i\mathbf{G}_{mnk} \cdot \mathbf{r}}, \quad (2.4)$$

where $|m| \leq N, |n| \leq N, |k| \leq N$, and $m, n, k \in \mathbb{Z}$. In this expansion, the number of Fourier components is $(2N + 1)^3$. The discussion in Sections 2.1 and 2.2 is based on the N modes expansion.

2.1. Given $\mathbf{b}_1, \mathbf{b}_2, \mathbf{b}_3$, generate $\{\phi(\mathbf{G})\}$

When given $\mathbf{b}_1, \mathbf{b}_2, \mathbf{b}_3$, the free energy density is just a function of $\{\phi(\mathbf{G})\}$. We can use optimization methods, like the conjugate gradient (CG) method, to generate $\{\phi(\mathbf{G})\}$, or we can use some non-linear equation system methods, like the Newton method, to solve the equation system generated from the necessary condition that the gradient vector is zero. The gradient vector is calculated by the following equation:

$$\frac{\partial F}{\partial \phi(\mathbf{G})} = [\xi^2 (1 - \mathbf{G}^2)^2 + \tau] \phi(\mathbf{G}) - \frac{\gamma}{2} \sum_{\mathbf{G}_1 + \mathbf{G}_2 = \mathbf{G}} \phi(\mathbf{G}_1) \phi(\mathbf{G}_2) + \frac{1}{6} \sum_{\mathbf{G}_1 + \mathbf{G}_2 + \mathbf{G}_3 = \mathbf{G}} \phi(\mathbf{G}_1) \phi(\mathbf{G}_2) \phi(\mathbf{G}_3). \quad (2.5)$$

No matter which method is selected to obtain $\{\phi(\mathbf{G})\}$, the gradient vector and the free energy must be calculated repeatedly. Note that calculating the gradient vector requires a lot of summations. These terms introduce great computational complexity if the method is not well designed. The main difficulty comes from valuating the term $\sum_{\mathbf{G}_1 + \mathbf{G}_2 + \mathbf{G}_3 = \mathbf{G}} \phi(\mathbf{G}_1) \phi(\mathbf{G}_2) \phi(\mathbf{G}_3)$. Given \mathbf{G} , if a simple cycle statement is used on $\mathbf{G}_1, \mathbf{G}_2$, the computational complexity is $O((2N + 1)^6)$, because $\mathbf{G}_1, \mathbf{G}_2$ iterate through all the $(2N + 1)^3$ Fourier components. In order to generate the gradient vector, \mathbf{G} iterates all the $(2N + 1)^3$ Fourier components as well. Using this approach, the computational complexity reaches $O((2N + 1)^9)$. We need to find another approach.

2.1.1. Calculating $\sum_{\mathbf{G}_1 + \mathbf{G}_2 + \mathbf{G}_3 = \mathbf{G}} \phi(\mathbf{G}_1) \phi(\mathbf{G}_2) \phi(\mathbf{G}_3)$ by FFT

Fortunately, the sum $\sum_{\mathbf{G}_1 + \mathbf{G}_2 + \mathbf{G}_3 = \mathbf{G}} \phi(\mathbf{G}_1) \phi(\mathbf{G}_2) \phi(\mathbf{G}_3)$ is actually a convolution sum, and calculating convolution sum is a well-known practice in spectral methods. The idea of the techniques is based on the fact that if $\{\phi(\mathbf{G})\}$ are Fourier coefficients of function $h(\mathbf{r})$, then $\sum_{\mathbf{G}_1 + \mathbf{G}_2 + \mathbf{G}_3 = \mathbf{G}} \phi(\mathbf{G}_1) \phi(\mathbf{G}_2) \phi(\mathbf{G}_3)$ are the Fourier coefficients of function $h^3(\mathbf{r})$. The key point in the techniques is how to avoiding the aliasing error. Two types of methods are developed to solve this problem. One is by padding or truncation, and another is by phase shifts.

In our code, we use the latter one. The detail of the techniques could be found on many books about spectral methods, see for example [3].

2.1.2. Optimization methods or non-linear equation system methods?

Either optimization methods or non-linear equation system methods can be used to solve $\{\phi(\mathbf{G})\}$. A disadvantage of non-linear equation system methods is that they need to calculate the Hessian matrix or an approximation of it, which increases the computational complexity to at least $O((2N+1)^6)$. Advantages include that they have quadratic convergence and they are easy to produce multiple solutions because they are sensitive to the initial value.

For optimization methods, disadvantages include slow speed of convergence and insensitivity to the initial value, so that they do not produce many solutions. An advantage is that some of them do not need the information of the Hessian matrix, an important example is the CG method, and this decreases the computational complexity.

No single method is best. when N is small, non-linear equation system methods are better; when N is large, optimization methods that don't need to calculate the Hessian matrix are better. This satisfies our goal of finding as many solutions as possible within manageable computational complexity.

2.2. Given $\{\phi(\mathbf{G})\}$ to get $\mathbf{b}_1, \mathbf{b}_2, \mathbf{b}_3$

If $\mathbf{b}_1, \mathbf{b}_2, \mathbf{b}_3$ are one of the solutions, the first derivatives of the free energy function with respect to b_{ij} , where $i, j = 1, 2, 3$, should be zero. We can choose a proper coordinate system such that $b_{12} = 0, b_{13} = 0, b_{23} = 0, b_{11} \neq 0, b_{22} \neq 0, b_{33} \neq 0$. We get

$$\sum_{m,n,k} \phi_{mnk}^2 (|\mathbf{G}_{mnk}|^2 - 1) m^2 = 0, \quad \sum_{m,n,k} \phi_{mnk}^2 (|\mathbf{G}_{mnk}|^2 - 1) mn = 0, \quad (2.6)$$

$$\sum_{m,n,k} \phi_{mnk}^2 (|\mathbf{G}_{mnk}|^2 - 1) mk = 0, \quad \sum_{m,n,k} \phi_{mnk}^2 (|\mathbf{G}_{mnk}|^2 - 1) n^2 = 0, \quad (2.7)$$

$$\sum_{m,n,k} \phi_{mnk}^2 (|\mathbf{G}_{mnk}|^2 - 1) nk = 0, \quad \sum_{m,n,k} \phi_{mnk}^2 (|\mathbf{G}_{mnk}|^2 - 1) k^2 = 0. \quad (2.8)$$

Expanding these expressions, the equations for the primitive reciprocal vectors are

$$b_1^2 \sum \phi_{mnk}^2 m^4 + 2b_1 b_2 \sum \phi_{mnk}^2 m^3 n + 2b_1 b_3 \sum \phi_{mnk}^2 m^3 k + b_2^2 \sum \phi_{mnk}^2 m^2 n^2 + 2b_2 b_3 \sum \phi_{mnk}^2 m^2 nk + b_3^2 \sum \phi_{mnk}^2 m^2 k^2 = \sum \phi_{mnk}^2 m^2, \quad (2.9)$$

$$b_1^2 \sum \phi_{mnk}^2 m^3 n + 2b_1 b_2 \sum \phi_{mnk}^2 m^2 n^2 + 2b_1 b_3 \sum \phi_{mnk}^2 m^2 nk + b_2^2 \sum \phi_{mnk}^2 mn^3 + 2b_2 b_3 \sum \phi_{mnk}^2 mn^2 k + b_3^2 \sum \phi_{mnk}^2 mnk^2 = \sum \phi_{mnk}^2 mn, \quad (2.10)$$

$$b_1^2 \sum \phi_{mnk}^2 m^3 k + 2b_1 b_2 \sum \phi_{mnk}^2 m^3 nk + 2b_1 b_3 \sum \phi_{mnk}^2 m^2 k^2 + b_2^2 \sum \phi_{mnk}^2 mn^2 k + 2b_2 b_3 \sum \phi_{mnk}^2 mnk^2 + b_3^2 \sum \phi_{mnk}^2 mk^3 = \sum \phi_{mnk}^2 mk, \quad (2.11)$$

$$b_1^2 \sum \phi_{mnk}^2 m^2 n^2 + 2b_1 b_2 \sum \phi_{mnk}^2 mn^3 + 2b_1 b_3 \sum \phi_{mnk}^2 mn^2 k + b_2^2 \sum \phi_{mnk}^2 n^4 + 2b_2 b_3 \sum \phi_{mnk}^2 n^3 k + b_3^2 \sum \phi_{mnk}^2 n^2 k^2 = \sum \phi_{mnk}^2 n^2, \quad (2.12)$$

$$b_1^2 \sum \phi_{mnk}^2 m^2 nk + 2b_1 b_2 \sum \phi_{mnk}^2 mn^2 k + 2b_1 b_3 \sum \phi_{mnk}^2 mnk^2 + b_2^2 \sum \phi_{mnk}^2 n^3 k + 2b_2 b_3 \sum \phi_{mnk}^2 n^2 k^2 + b_3^2 \sum \phi_{mnk}^2 nk^3 = \sum \phi_{mnk}^2 nk, \quad (2.13)$$

$$b_1^2 \sum \phi_{mnk}^2 m^2 k^2 + 2b_1 b_2 \sum \phi_{mnk}^2 mnk^2 + 2b_1 b_3 \sum \phi_{mnk}^2 mk^3 + b_2^2 \sum \phi_{mnk}^2 n^2 k^2 + 2b_2 b_3 \sum \phi_{mnk}^2 nk^3 + b_3^2 \sum \phi_{mnk}^2 k^4 = \sum \phi_{mnk}^2 k^2. \quad (2.14)$$

Though the above six equations are non-linear with respect to $\mathbf{b}_1, \mathbf{b}_2, \mathbf{b}_3$, they are linear equations for $\mathbf{b}_1^2, \mathbf{b}_2^2, \mathbf{b}_3^2, \mathbf{b}_1 \mathbf{b}_2, \mathbf{b}_1 \mathbf{b}_3, \mathbf{b}_2 \mathbf{b}_3$. Once $\mathbf{b}_1^2, \mathbf{b}_2^2, \mathbf{b}_3^2, \mathbf{b}_1 \mathbf{b}_2, \mathbf{b}_1 \mathbf{b}_3, \mathbf{b}_2 \mathbf{b}_3$ are solved, $\mathbf{b}_1, \mathbf{b}_2, \mathbf{b}_3$ can also be determined.

Now, for a given N , we can obtain $\phi^{(N)}(\mathbf{r})$ and $\mathbf{b}_1, \mathbf{b}_2, \mathbf{b}_3$ according to the iteration process, hereafter referred to as Procedure I, which is specified in the following four steps.

- Step 1. Given an initial value $\{\phi(\mathbf{G})\}$, $\mathbf{b}_1, \mathbf{b}_2, \mathbf{b}_3$ and set $m = 1$, then calculate the free energy density f_m .
- Step 2. Fixed $\mathbf{b}_1, \mathbf{b}_2, \mathbf{b}_3$, calculate $\{\phi(\mathbf{G})\}$ by the method described in Section 2.1.
- Step 3. Adjust $\mathbf{b}_1, \mathbf{b}_2, \mathbf{b}_3$ by the method described in Section 2.2.
- Step 4. Calculate the free energy density f_{m+1} , if $|f_{m+1} - f_m| > \epsilon$, then set $f_m = f_{m+1}$, $m = m + 1$, go back to step 2.

2.3. The way to find appropriate N and good initial estimate of $\{\phi(\mathbf{G})\}$

Now, Procedure I can be applied to calculate $\phi^{(N)}(\mathbf{r})$ for given N . However, new problems arise. Because $\phi^{(N)}(\mathbf{r})$ is just an estimate of $\phi(\mathbf{r})$, the first problem is, how large is enough for N to make $\phi^{(N)}(\mathbf{r})$ a good estimate of $\phi(\mathbf{r})$? If N is too large, the computational complexity may go beyond the computer's capacity; if N is too small, $\phi^{(N)}(\mathbf{r})$ may be far away from $\phi(\mathbf{r})$. Since both the optimization methods and the non-linear equation system methods are sensitive to the initial value, bad initial estimate will slow down the convergence speed of Process I. The second problem is how to give a good initial value of $\{\phi(\mathbf{G})\}$ and $\mathbf{b}_1, \mathbf{b}_2, \mathbf{b}_3$ in step 1 of Process I for a given N . The following process, referred to as Procedure II, is used to overcome the two problems.

- Step 1. Starting from $N = 1$, generate an initial estimate of $\phi(\mathbf{G}_{mnk})$ and $\mathbf{b}_1, \mathbf{b}_2, \mathbf{b}_3$ randomly, where $\{m, n, k\} \in \{-1, 0, 1\}$, and apply Procedure I to generate $\phi^{(1)}(\mathbf{r})$ and $\mathbf{b}_1, \mathbf{b}_2, \mathbf{b}_3$, and the free energy density value $f(\phi^{(1)}(\mathbf{r}), \mathbf{b}_1, \mathbf{b}_2, \mathbf{b}_3)$.
- Step 2. Use $\phi^{(1)}(\mathbf{r})$ and $\mathbf{b}_1, \mathbf{b}_2, \mathbf{b}_3$ as the initial estimate of 2 modes problem, and then apply Procedure I to generate $\phi^{(2)}(\mathbf{r})$, the corresponding $\mathbf{b}_1, \mathbf{b}_2, \mathbf{b}_3$, and the free energy density $f(\phi^{(2)}(\mathbf{r}), \mathbf{b}_1, \mathbf{b}_2, \mathbf{b}_3)$.
- Step 3. Repeat the above two steps till

$$|f(\phi^{(N)}(\mathbf{r}), \mathbf{b}_1, \mathbf{b}_2, \mathbf{b}_3) - f(\phi^{(N-1)}(\mathbf{r}), \mathbf{b}_1, \mathbf{b}_2, \mathbf{b}_3)| < \epsilon.$$

By executing Procedure II hundreds of times, different equilibrium phases can be discovered. For the first problem, a clear constraint is defined: the N , which makes the difference of the free energy density between N modes and $(N - 1)$ modes less than an given small number ϵ , is the appropriate one. For the second problem, the solutions of $(N - 1)$ modes are used as the initial estimate of N modes; while for the situation $N = 1$, because the computational complexity is small, a lot of randomly chosen initial estimates are allowed.

Though all the above discussion is based on the three-dimensional problem, the whole process can be adapted directly to two-dimensional and 1-dimensional problems.

3. Numerical results

3.1. Efficiency

We are going to depict the efficiency of the method from two points of view. First we will consider the time and the number of modes to convergence for one set of ξ, τ and γ , then we will compare the phase diagram with the former results.

3.1.1. For one set of ξ, τ and γ

In this test, the Newton method for non-linear systems was used to calculate the $\phi^{(N)}(\mathbf{r})$ when $N \leq 2$; the CG method was used for the other cases. The ϵ in Procedure II was set to 10^{-6} , and $\xi = 1.0, \tau = -1.0, \gamma = 0.6$. Procedure II was run 100 times on a Pentium(R) 4 3.00 GHz CPU with memory 1 G. Each time the initial value of $\phi(\mathbf{G})$ and $\mathbf{b}_1, \mathbf{b}_2, \mathbf{b}_3$ was randomly chosen for $N = 1$. Because the speed of convergence depends on the initial value, the time and the modes to convergence are different for different initial value. Fig. 1 shows that, in these 100 runs, the average time to convergence was 38.4249 s, while the maximum was 490 s; the aver-

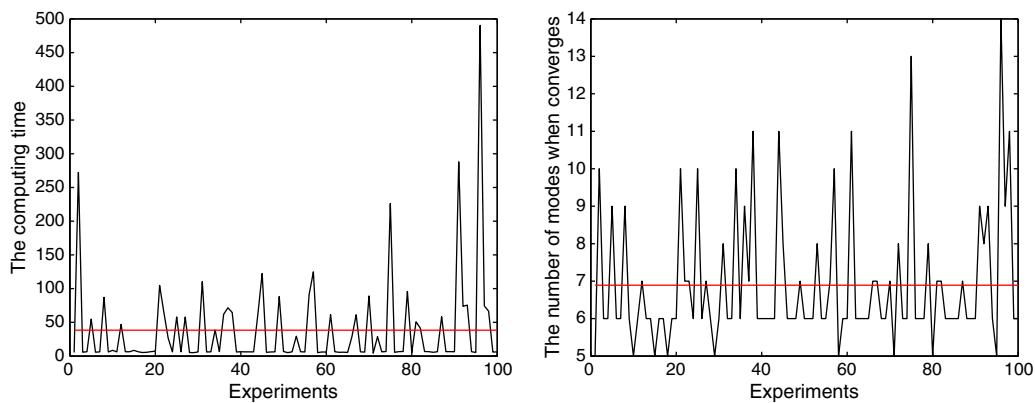


Fig. 1. The time to convergence and the modes to converge in 100 runs. The flat line shows the average.

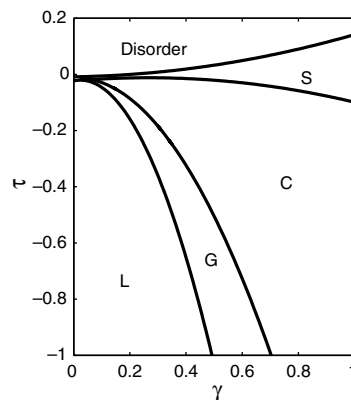


Fig. 2. The phase diagram when $\xi = 1.0$. S, C, G and L represent sphere phase, cylinder phase, gyroid phase and lamellar phase, respectively.

age modes to convergence was 7, while the maximum was 14. Even in the worst case, where Procedure II converged on 14 modes, which required the calculation of $(2 \times 14 + 1)^3 - 1 = 24389$ variables, the time to convergence remained a manageable 490 s.

3.1.2. Phase diagram when $\xi = 1.0$

Using the Landau–Brazovskii model, Podnicksa and Hamley [15] calculated the phase diagram using a limited number of basis functions. Shi [13] plotted a more accurate phase diagram by expanding the order parameter into more basis functions. Fig. 2 shows the phase diagram generated by our method, which is consistent with both Podnicksa and Hamley’s and Shi’s results.

3.2. Some meta-stable phases

Because our method does not need any a priori information about symmetry, and different initial estimates may converge to different solutions, both stable and meta-stable phases can be captured.

To illustrate this point, we will select some points in the phase diagram as examples. Fig. 3 shows three phases when $\xi = 1.0$, $\tau = -1.0$, $\gamma = 0.6$. The stable phase is gyroid phase as shown at the left, and perforated-lamellar and double diamond phases are the meta-stable phases shown at the right.

Some new morphologies are also generated by our method, but, unfortunately, they are all meta-stable phases. The left image in Fig. 4 shows a new phase when $\xi = 1.0$, $\tau = -1.0$, $\gamma = 0.6$. The element of the structure is a piece of “snow” with six arms. Three of them bend up while the other three bend down. A new phase

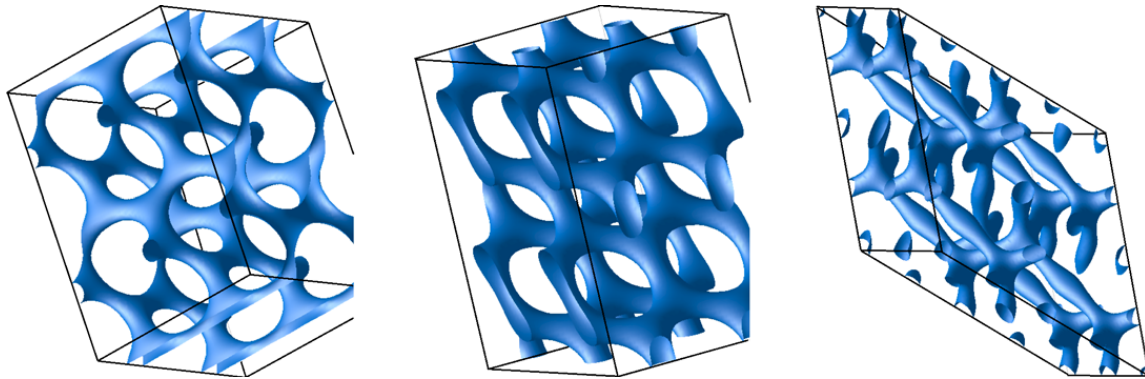


Fig. 3. The gyroid, the perforated-lamellar and double-diamond phase when $\xi = 1.0$, $\tau = -1.0$, $\gamma = 0.60$. In this case, the gyroid is stable phase; the other two are meta-stable phases.

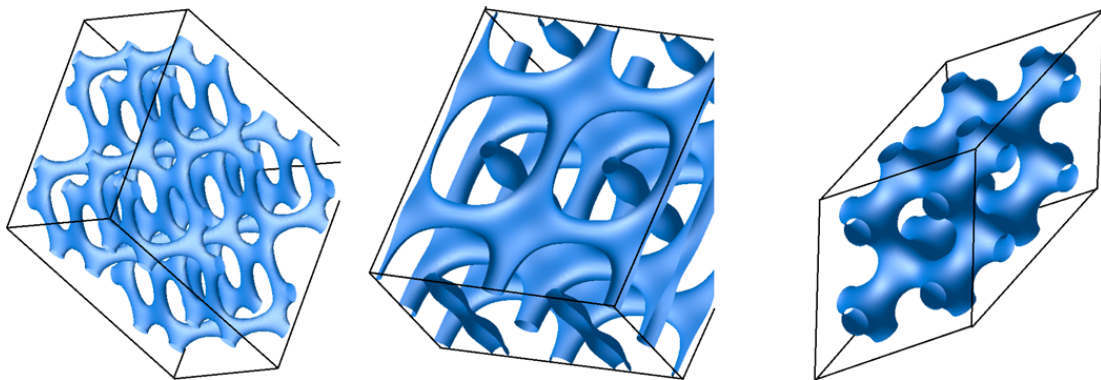


Fig. 4. From left to right, three new phases generated by the method when $\xi = 1.0$, $\tau = -1.0$, $\gamma = 0.6$; $\xi = 1.0$, $\tau = -1.0$, $\gamma = 0.78$; and $\xi = 1.0$, $\tau = -0.32$, $\gamma = 0.34$, respectively.

is shown in the middle of Fig. 4 when $\xi = 1.0$, $\tau = -1.0$, $\gamma = 0.78$. The structure is constructed by pillars going across layers. The right diagram in Fig. 4 shows a new phase when $\xi = 1.0$, $\tau = -0.32$, $\gamma = 0.34$. This phase is similar to the perforated-lamellar phase, but the layers are interconnected.

The existence of the new phases remains to be observed in experiments. Since they are meta-stable phases, they are probably difficult to observe.

3.3. The epitaxial relationship between cylinder and lamellar, and between cylinder and sphere

Masten [14] studied the mechanism of the phase transition from cylinder phase to sphere phase. If D_c denotes the period of the cylinder phase, and D_s denotes the distance between two adjacent spheres along the direction $[1, 1, 1]$, Masten assumed that $D_c = \sqrt{8}/3D_s$. Because the period vectors are adjusted during the iteration in our method, we tried to confirm the epitaxial relationship numerically. We selected samples along the line $\gamma = 1.0$, and calculated the relative error between D_c and $\sqrt{8}/3D_s$. The relative error is at most 0.63% as shown in Table 1, so it is reasonable to believe the relationship $D_c = \sqrt{8}/3D_s$ is correct.

Table 1
The relationship between D_s and D_c at some samples along line $\gamma = 1.0$

γ	τ	D_s	$\sqrt{8}/3D_s$	D_c	Error($ D_c - \sqrt{8}/3D_s /D_c$) (%)
1.00	0.00	7.811968	7.365194	7.318730	0.63
1.00	-0.20	7.808210	7.361651	7.318544	0.59
1.00	-0.40	7.805536	7.359130	7.318098	0.56
1.00	-0.60	7.803437	7.357151	7.317472	0.54
1.00	-0.80	7.800685	7.354556	7.316719	0.52
1.00	-1.00	7.797738	7.351778	7.315881	0.49
1.00	-1.20	7.797050	7.351129	7.314991	0.49

Table 2

The relationship between D_1 and D_c at samples along line $\tau = -0.8$

γ	τ	D_1	$2/\sqrt{3}D_1$	D_c	Error($(D_c - 2/\sqrt{3}D_1 /D_c)$ (%)
0.30	-0.80	6.301395	7.276224	7.332815	0.77
0.32	-0.80	6.303428	7.278572	7.325534	0.64
0.34	-0.80	6.305607	7.281088	7.410549	1.75
0.36	-0.80	6.307937	7.283778	7.315266	0.43
0.38	-0.80	6.310421	7.286647	7.311638	0.34
0.40	-0.80	6.313063	7.289697	7.308740	0.26
0.42	-0.80	6.315868	7.292936	7.328141	0.48

Wickham et al. [16] did some work on the nucleation from the meta-stable lamellar phase to the stable cylinder phase. They assumed an epitaxial relation of $D_c = 2/\sqrt{3}D_1$, where D_1 is the distance between two adjacent layers, D_c is the period of the cylinder phase. Again, our numerical method can examine their assumption. Table 2 shows the results of several samples along the line $\tau = -0.80$. The relative error between D_c and $2/\sqrt{3}D_1$ is at most 1.75%, which is at a reasonable level.

3.4. The situation when ξ is small

The above numerical results are based on the condition $\xi = 1.0$, and the Procedure II always converges. This means there always exists period vectors a_1, a_2, a_3 such that the free energy density function reaches its minimum point. What is the situation when ξ is small?

As shown in Section 3.2, when $\xi = 1.0$, $\tau = -1.0$, and $\gamma = 0.6$, the gyroid phase is the stable phase, the perforated-lamellar phase, double-diamond phase, and one new phase are meta-stable. Keeping τ and γ the same, and changing the ξ to 0.2, Procedure II could not converge even the number of modes reaches 30. As the number of the modes increases, the length of the period also increases, and gives no evidence of convergence. Fig. 5 shows the relationship between the number of modes and the length of a_1, a_2 and a_3 .

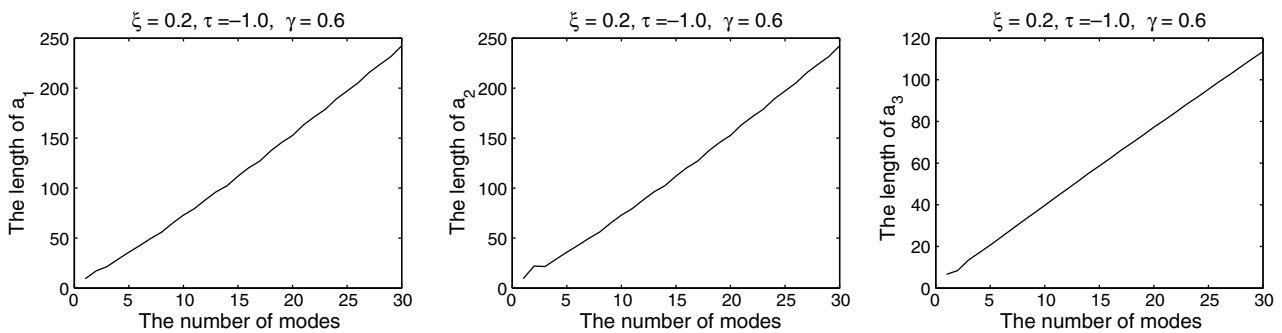


Fig. 5. From left to right, the relationship between the number of modes and the length of a_1 , a_2 and a_3 when $\xi = 0.2$, $\tau = -1.0$, $\gamma = 0.6$.

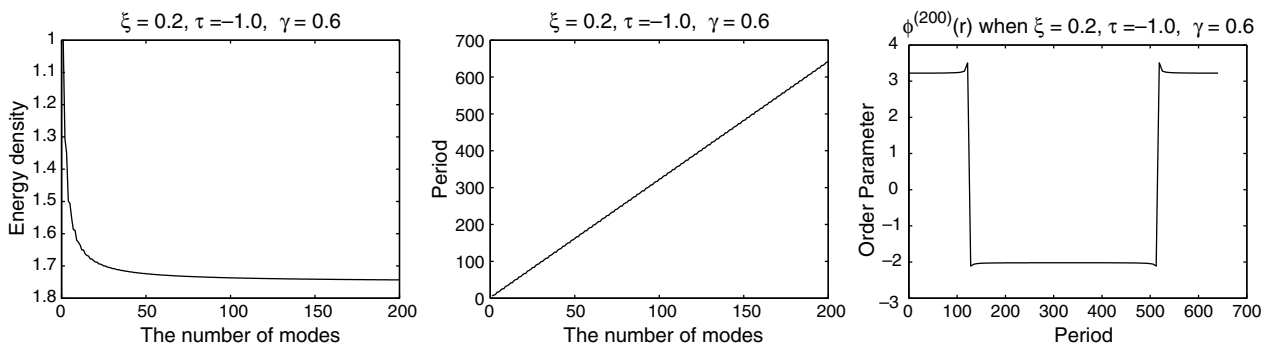


Fig. 6. From left to right, the relationship between the free energy density and the number of modes, between the period and the number of modes, the profile of $\phi^{(200)}(\mathbf{r})$, when $\xi = 0.2$, $\tau = -1.0$, $\gamma = 0.6$.

Because of the complexity of the 3-D problem, we reduce the problem to the 1-D case. Choosing the same parameters $\xi = 0.2$, $\tau = -1.0$ and $\gamma = 0.6$, we calculated up to 200 modes. The same phenomenon appears, Procedure II could not converge and the period increases as the number of modes moves up. Fig. 6 shows the relationship between the energy and the number of modes, the period and the number of modes, and the profile of $\phi^{(200)}(\mathbf{r})$.

Now keep τ and γ as the same, same calculation was executed to the situations $\xi = 0.02$, and $\xi = 0.002$ respectively. Because the results are almost the same, only the result for the case $\xi = 0.002$ is shown in Fig. 7.

As the number of modes increases, the free energy density has the tendency to converge, but the period shows no evidence to converge, and it is approximate a linear function with respect to the number of modes. As ξ decreases, the profile of the order parameter converges to a step function.

We conclude that, under the framework of the Landau–Brazovskii model, when ξ is small, the diblock copolymer system would rather have a macro separation instead of a micro separation. This is not reasonable because only microstructures can form for the diblock copolymer system. Therefore, Landau–Brazovskii model does not explain the physical phenomena when ξ is small.

We will try to find the limit of the order parameter $\phi(\mathbf{r})$ as ξ tends to zero. It is appropriate to assume that the order parameter is going to converge to the solution of the case $\xi = 0$. When $\xi = 0$, the free energy density functional becomes

$$f(\phi(\mathbf{r}))|_{\xi=0} = \frac{1}{V} \int_{\Omega} d\mathbf{r} \left\{ \frac{\tau}{2} [\phi(\mathbf{r})]^2 - \frac{\gamma}{3!} [\phi(\mathbf{r})]^3 + \frac{1}{4!} [\phi(\mathbf{r})]^4 \right\}. \quad (3.1)$$

For this case, we will find the minimum point in another way. Our goal is to find $\phi(\mathbf{r})$ such that the free energy density reaches its minimum under the constraint $\int d\mathbf{r} \phi(\mathbf{r}) = 0$. For fixed period, we introduce auxiliary functional

$$L(\phi(\mathbf{r}), \lambda) = f(\phi(\mathbf{r}))|_{\xi=0} - \frac{\lambda}{V} \int_{\Omega} d\mathbf{r} \phi(\mathbf{r}). \quad (3.2)$$

The solution satisfies

$$\frac{\partial L(\phi(\mathbf{r}), \lambda)}{\partial \lambda} = 0, \quad (3.3)$$

$$\frac{\delta L(\phi(\mathbf{r}), \lambda)}{\delta \phi(\mathbf{r})} = 0. \quad (3.4)$$

Eq. (3.3) is the constraint, while Eq. (3.4) is

$$\tau \phi(\mathbf{r}) - \frac{\gamma}{2} \phi(\mathbf{r})^2 + \frac{1}{6} \phi(\mathbf{r})^3 - \lambda = 0. \quad (3.5)$$

For every r_0 , $\phi(r_0)$ is a root of the polynomial Eq. (3.5). As the result of the constraint $\int d\mathbf{r} \phi(\mathbf{r}) = 0$, $\phi(\mathbf{r})$ has to be a step function with the following form:

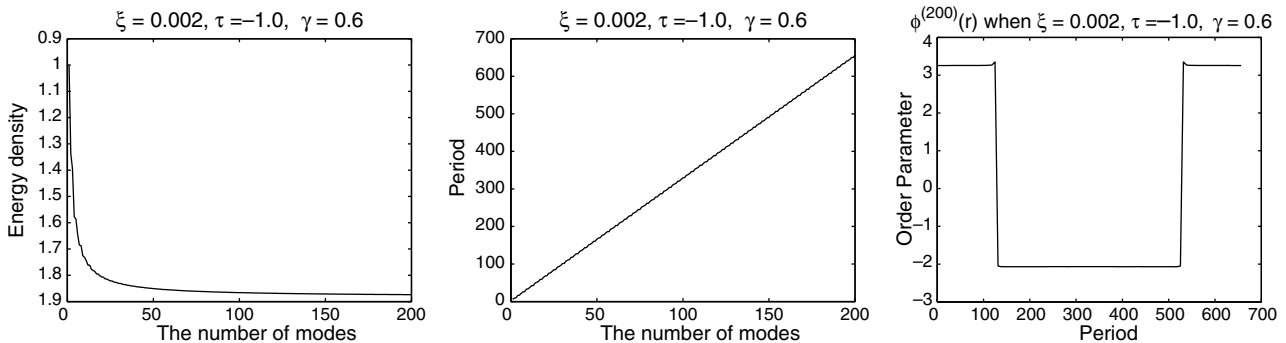


Fig. 7. From left to right, the relationship between the free energy density and the number of modes, between the period and the number of modes, the profile of $\phi^{(200)}(\mathbf{r})$, when $\xi = 0.002$, $\tau = -1.0$, $\gamma = 0.6$.

$$\phi(\mathbf{r}) = \begin{cases} x_1 > 0, & \text{in a block with length } \frac{-x_2}{x_1 - x_2} V \\ x_2 < 0, & \text{in a block with length } \frac{x_1}{x_1 - x_2} V \end{cases}, \quad (3.6)$$

where x_1, x_2 are the roots of Eq. (3.5), and they are essentially functions of λ . By substituting (3.6) into the free energy density function, and using the fact that

$$\tau x_i - \frac{\gamma}{2} x_i^2 + \frac{1}{6} x_i^3 - \lambda = 0, \quad \text{where } i \in \{1, 2\}, \quad (3.7)$$

the free energy density becomes a function of λ ,

$$f(\lambda) = -x_1 x_2 \left(\frac{\tau}{4} - \frac{\gamma^2}{8} \right) - \frac{\gamma \lambda}{4}. \quad (3.8)$$

We need to find λ to minimize $f(\lambda)$, then calculate the corresponding $\phi(\mathbf{r})$. We give a specific example when $\xi = 0.0$, $\tau = -1.0$, $\gamma = 0.6$. Fig. 8 shows the relationship between λ and $f(\lambda)$.

The free energy density hits its minimum point -1.8816 when $\lambda = -0.6720$. At this point, the positive part of $\phi(\mathbf{r})$ equals 3.2608 , and the negative part of $\phi(\mathbf{r})$ equals -2.0608 . Because the whole deduction is not related to the period, this $\phi(\mathbf{r})$ is the solution for any period when $\xi = 0.0$, $\tau = -1.0$, $\gamma = 0.6$.

Fig. 9 shows the profile of $\phi(\mathbf{r})$ when the period equals 680. We conclude that when ξ converges to zero, $\phi(\mathbf{r})$ is going to be a step function with positive part tends to 3.2608 and negative part tends to -2.0608 for the case $\xi = 0.0$, $\tau = -1.0$, $\gamma = 0.6$.

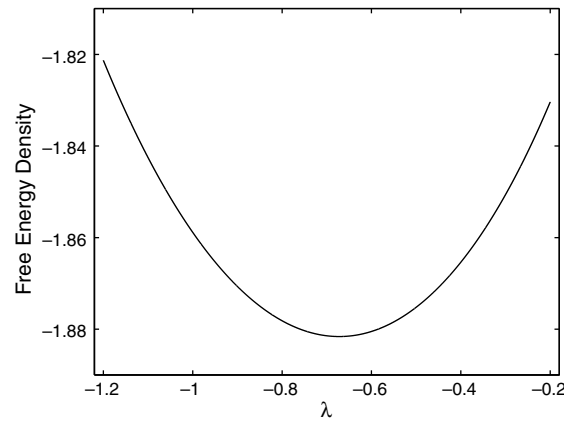


Fig. 8. The relationship between λ and the free energy density.

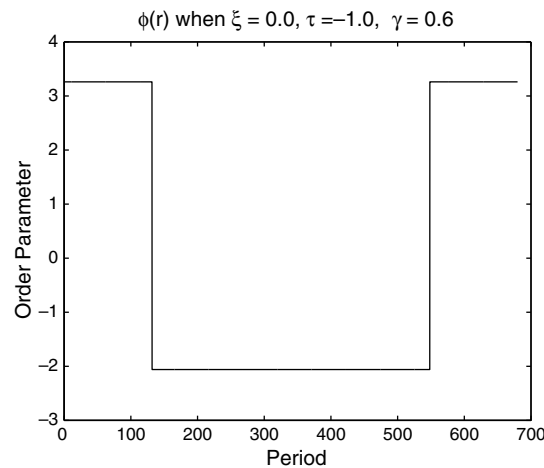


Fig. 9. The profile of $\phi(\mathbf{r})$, when $\xi = 0.0$, $\tau = -1.0$, $\gamma = 0.6$.

4. Conclusion

Based on the Landau–Brazovskii model, a new efficient numerical method which does not need a priori symmetric information and, more significantly, can adjust the period structure automatically has been developed. The way to generate good initial estimates is well defined as well. The phase diagram generated by the method proved the correctness of the method. Using this method, we can calculate not only the stable phase, but also the meta-stable phases. Without the assumption of symmetry, the method can discover new phases as well as the typical sphere, cylinder, lamellar, gyroid, perforated-lamellar and double-diamond phases. Three new meta-stable phases have been investigated, but the existence need to be proved by experiments. The epitaxial relation in the phase transition can also be numerically validated using the method. We found the Landau–Brazovskii model could not explain the physical phenomena when ξ is small, because the diblock copolymer system would rather have a macro separation instead of a micro separation under the framework of Landau–Brazovskii model. Our future work will focus on SCFT, and we will try to add the period structure into SCFT to develop a method which can adjust them automatically as what we have done on the platform based on Landau–Brazovskii model.

Acknowledgments

The authors would like to acknowledge Prof. An-chang Shi for the help on understanding the Landau–Brazovskii model and SCFT; Dr. Sharon Murrel for the help on the english writing; Bachelor Meng Yu for the debate on 1-D problem. This work is supported by the special funds for Major State Research Projects 2005CB321704, and National Science Foundation of China for Distinguished Young Scholars 10225103 and 20490222.

References

- [1] M.W. Matsen, The standard Gaussian model for block copolymer melts, *J. Phys.: Condens. Matter* 14 (2002) R21–R47.
- [2] M. Doi, S.F. Edwards, *The Theory of Polymer Dynamics*, Clarendon Press, Oxford, 2002.
- [3] C.G. Canuto, M.Y. Hussaini, A. Quarteroni, T.A. Zang, *Spectral Methods in Fluid Dynamics*, Springer-Verlag, 1988.
- [4] E. Helfand, Theory of inhomogeneous polymers: fundamentals of the Gaussian random-walk model, *J. Chem. Phys.* 62 (1975) 999.
- [5] E. Helfand, Block copolymer theory. III. Statistical mechanics of the microdomain structure, *Macromolecules* 8 (1975) 552.
- [6] L. Leibler, Theory of Microphase Separation in Block Copolymers, *Macromolecules* 13 (1980) 1602.
- [7] S.A. Brazovskii, Phase transition of an isotropic system to a nonuniform state, *Sov. Phys.-JETP* 41 (1975) 85.
- [8] G.H. Fredrickson, E. Helfand, Fluctuation effects in the theory of microphase separation in block copolymers, *J. Chem. Phys.* 87 (1987) 697.
- [9] M.W. Matsen, M. Schick, Stable and unstable phases of a diblock copolymer melt, *Phys. Rev. Lett* 72 (1994) 2660.
- [10] F. Drolet, G.H. Fredrickson, Combinatorial screening of complex block copolymer assembly with self-consistent field theory, *Phys. Rev. Lett* 83 (1999) 4317.
- [11] G. Tzeremes, K.Ø. Rasmussen, T. Lookman, A. Saxena, Efficient computation of the structural phase behavior of block copolymers, *Phys. Rev. E* 65 (2002) 041806.
- [12] A.C. Shi, J. Noolandi, R.C. Desai, Theory of anisotropic fluctuations in ordered block copolymer phases, *Macromolecules* 29 (1996) 6487.
- [13] A.C. Shi, Nature of anisotropic fluctuation modes in ordered systems, *J. Phys.: Condens. Matter* 11 (1999) 10183.
- [14] M.W. Matsen, Cylinder↔sphere epitaxial transitions in block copolymer melts, *J. Chem. Phys.* 114 (2001) 8165.
- [15] V.E. Podnepska, I.W. Hamley, Landau–Brazovskii model for the Ia3d structure, *JETP Lett.* 64 (1996) 618.
- [16] R.A. Wickham, A.C. Shi, Z.G. Wang, Nucleation of stable cylinders from a metastable lamellar phase in a diblock copolymer melt, *J. Chem. Phys.* 118 (2003) 10293.